Supporting Information

High-Performance Stretchable Thermoelectric Multilayers Enabled by a Synergistic Elastomer-Conjugated Network

*Seok Hoon Lim,[a] Mario Culebras,[b] Yong Tae Park, *[c] Jung Sang Cho*[d] and Chungyeon Cho*[ae]*

[a] Department of Carbon Convergence Engineering, College of Engineering, Wonkwang University, Iksan, 54538, Republic of Korea

[b] Institute of Materials Science (ICMUV) Catedrático José Beltrán, 2, Paterna, València 46980, Spain

[c] School of Mechanical Systems Engineering, Myongji University, 116 Myongji-ro, Cheoin-gu, Yongin, Gyeonggi 17058, Republic of Korea

[d] Department of Engineering Chemistry, Chungbuk National University, Chungbuk, 361-763, Republic of Korea

[e] Department of Biomedical Materials Science, Jeonbuk Advanced Bio-convergence Academy, Wonkwang University, Iksan, Jeonbuk 54538, Republic of Korea

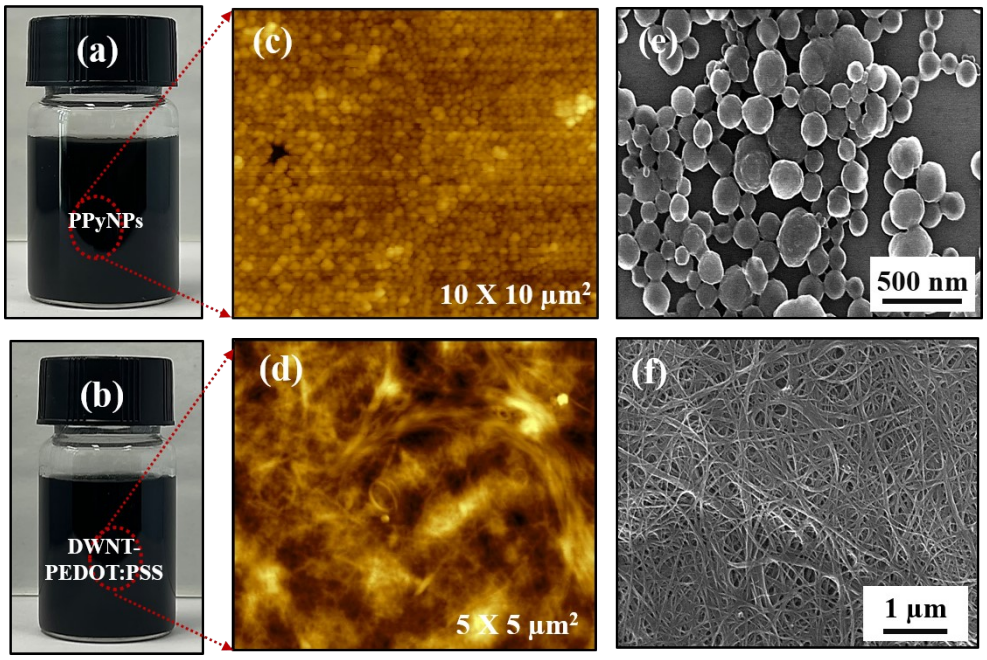

Fig. S1 Photo-images of the glass vials containing (a) PPyNPs and (b) DWNT-PEDOT:PSS solution and corresponding AFM ((c) and (d)) and SEM ((e) and (f)) images captured from Si-wafers of drop-cast each solution.

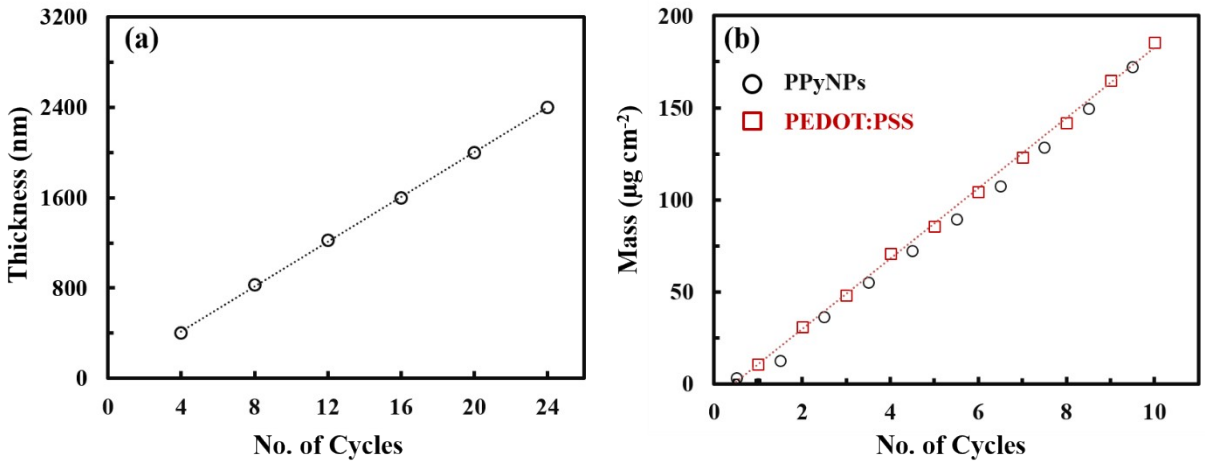

Fig. S2 (a) Profilometer measured thickness on a Si-wafer and (b) mass of PPyNPs/PEDOT:PSS LbL thin films as a function of bilayers deposited.

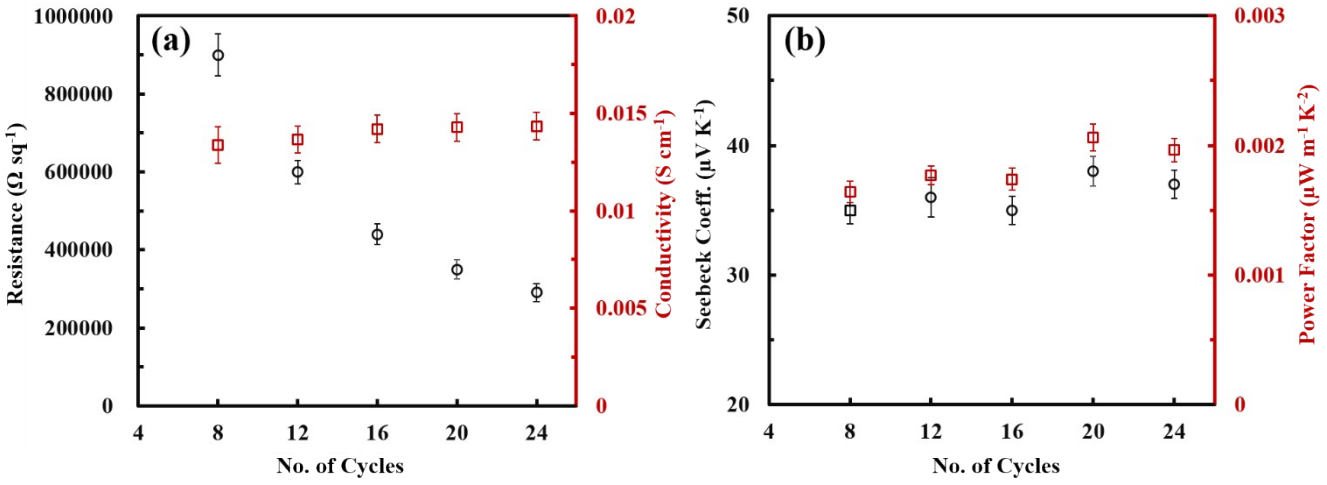

Fig. S3 (a) Sheet resistance (circle) and electrical conductivity (square) and (b) Seebeck coefficient (circle) and power factor (square) of PPyNPs/PEDOT:PSS LbL thin films deposited on PET substrates as a function of the number of deposition cycles.

Table S1 Valence band edge and work function calculated for PPyNPs/DWNT-PEDOT:PSS LbL thin films with the number of layers deposited on Si-wafers. HOMO edges and work functions were calculated by using previously reported methods [1-3].

LbL assemblies	$E_{HOMO, onset}$ (eV)	Work function (eV)
12 BL	4.34	3.25
16 BL	4.51	3.67
20 BL	4.56	3.88

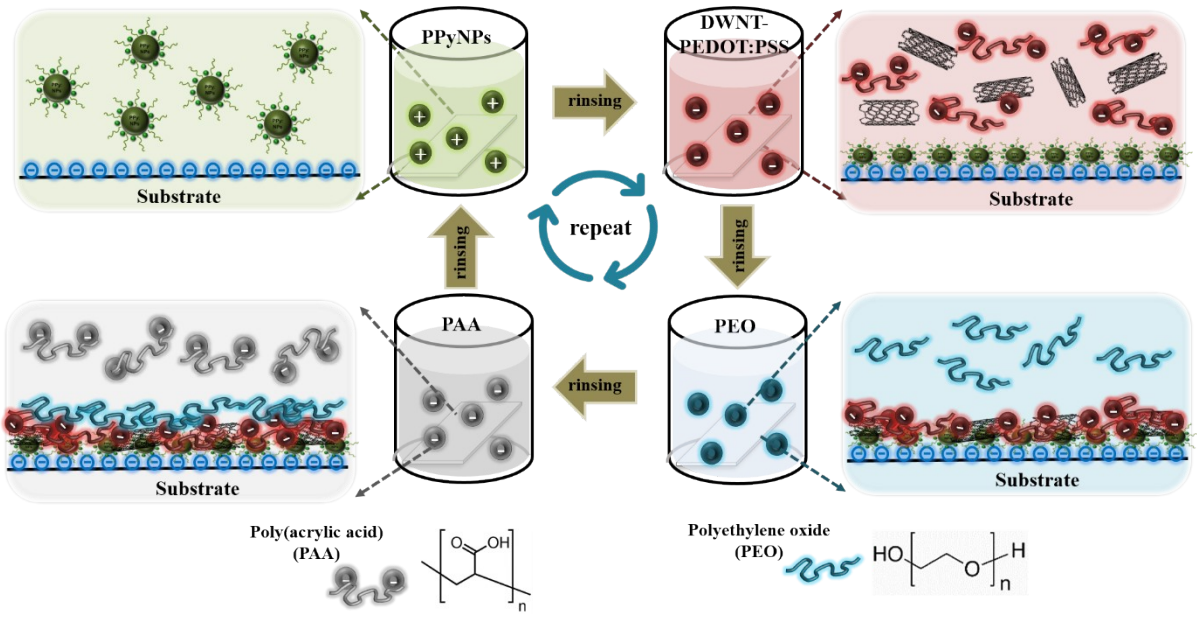

Fig. S4 Schematic of the layer-by-layer (LbL) assembly of stretchable thermoelectric quadlayer films composed of PPyNPs, DWNT-PEDOT:PSS, PEO, and PAA. PPyNPs act as p-type conducting nanoparticles, DWNT-PEDOT:PSS provides conjugated conductive pathways, and PEO/PAA serve as flexible binders, together forming robust and stretchable multilayer architectures.

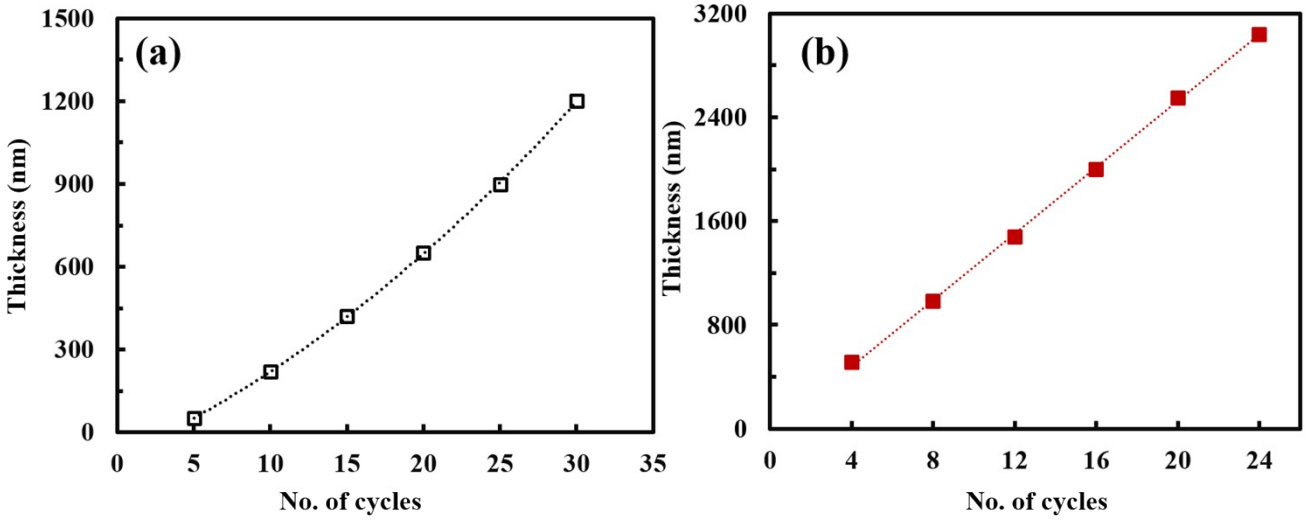

Fig. S5 Profilometer thickness of (a) PEO/PAA and (b) PPyNPs/DWNT-PEDOT:PSS/PEO/PAA films grown on Si-wafers as a function of cycles deposited.

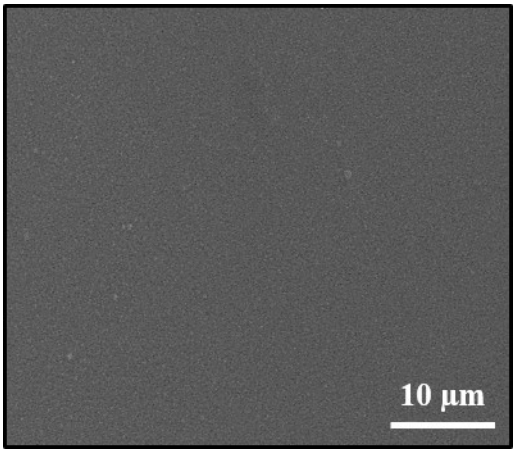

Fig. S6 SEM image of PEO/PAA films showing a featureless and smooth surface, characteristic of soft elastomeric morphology before strain.

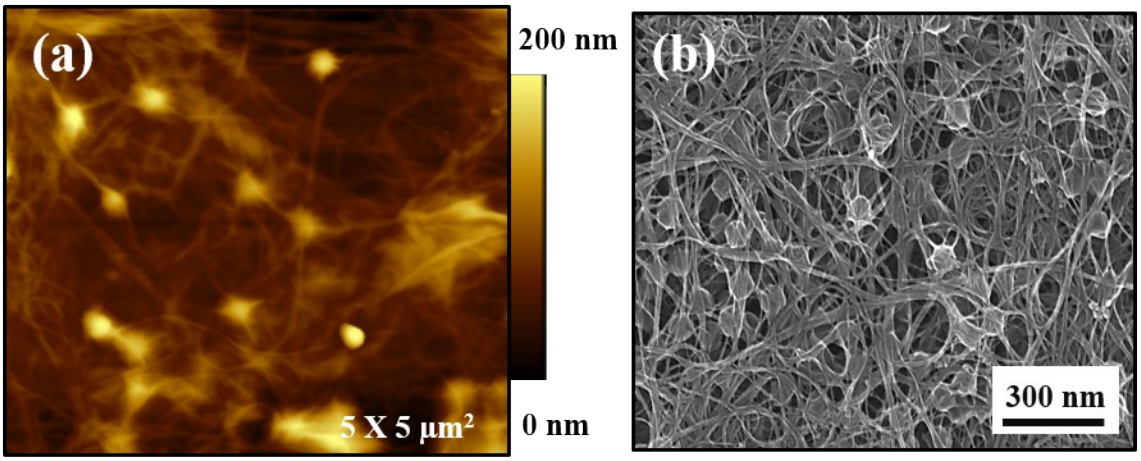

Fig. S7 (a) AFM and (b) SEM images of PPyNPs/DWNT-PEDOT:PSS/PEO/PAA QL films, confirming that incorporation of PEO/PAA does not disrupt the conjugated nanostructure.

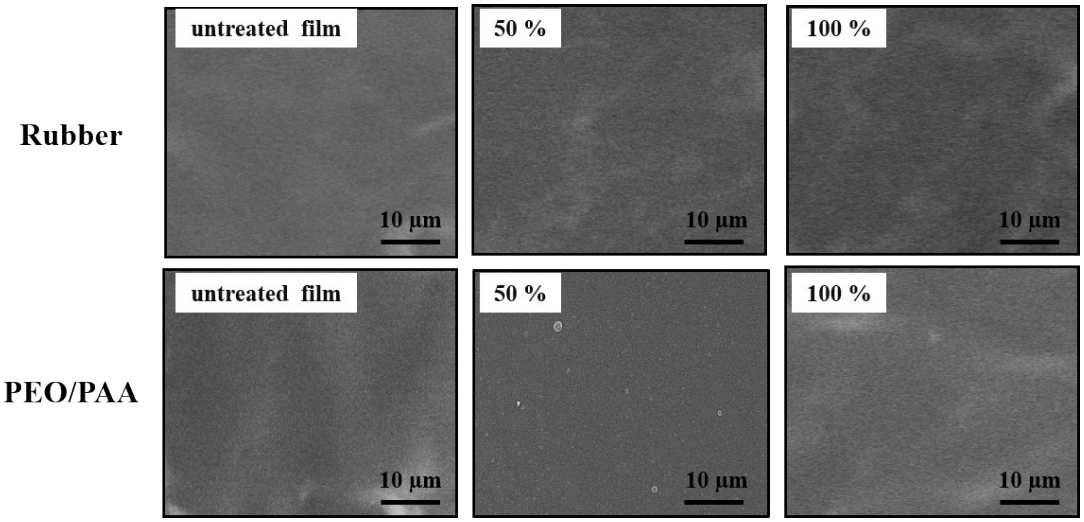

Fig. S8 SEM images of PU rubber and PEO/PAA-coated PU before and after stretching, demonstrating crack-free morphology even beyond 100% strain.

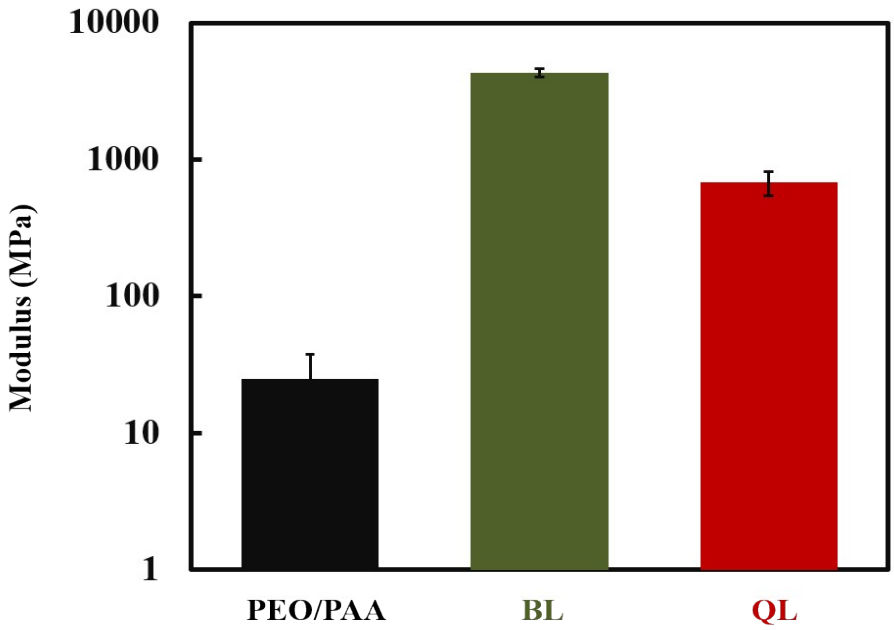

Fig. S9 Elastic modulus of 20 PEO/PAA, PPyNPs/DWNT-PEDOT:PSS BL and PPyNPs/DWNT-PEDOT:PSS/PEO/PAA QL films deposited on a Si-wafer.

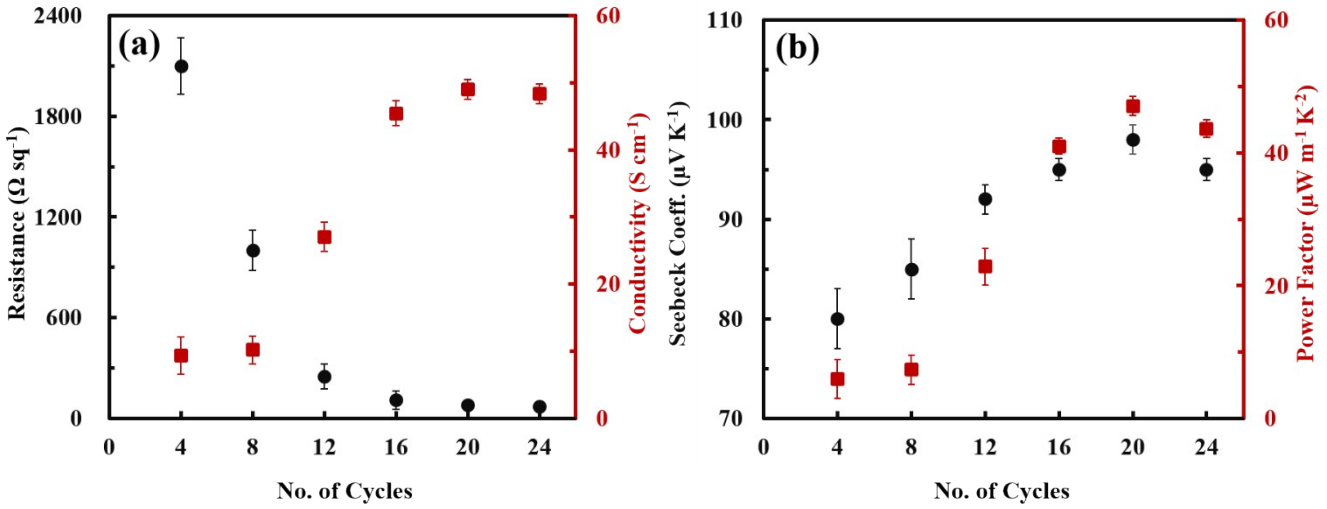

Fig. S10 (a) Sheet resistance (circle) and electrical conductivity (square) and (b) Seebeck coefficient (circle) and power factor (square) of PPyNPs/DWNT-PEDOT:PSS/PEO/PAA LbL thin films deposited on PET substrates as a function of the number of deposition cycles.

References

[1] D. L. Stevens, A. Parra, J. C. Grunlan, Thermoelectric Performance Improvement of Polymer Nanocomposites by Selective Thermal Degradation. ACS Appl. Energy Mater. 2 (2019) 5975-5982.

[2] A. Kahn, Fermi Level, Work Function and Vacuum Level. Mater. Horiz. 3 (2016) 7-10.

[3] S. L. Kim, K. Choi, A. Tazebay, C. Yu, Flexible Power Fabrics Made of Carbon Nanotubes for Harvesting Thermoelectricity. ACS Nano 8 (2014) 2377-2386.